Control of emitted light polarization in a 1310 nm dilute nitride spin-Vertical Cavity Surface Emitting Laser subject to circularly-polarized optical injection

S.S. Alharthi[1], A. Hurtado[1], R.K. Al Seyab[1], V.-M. Korpijarvi[2], M. Guina[2], I.D. Henning[1] and M.J. Adams[1]

[1]*School of Computer Science and Electronic Engineering, University of Essex, Wivenhoe Park, Colchester, CO4 3SQ, United Kingdom.*

[2]*Optoelectronics Research Centre (ORC), Tampere University of Technology, P.O. Box 692, FIN-33101 Tampere, Finland*

**ssmalh@essex.ac.uk*

We experimentally demonstrate the control of the light polarization emitted by a 1310 nm dilute nitride spin-Vertical Cavity Surface Emitting Laser (VCSEL) at room temperature. This is achieved by means of a combination of polarized optical pumping and polarized optical injection. Without external injection the polarization of the optical pump controls that of the spin-VCSEL. However, the addition of the externally injected signal polarized with either left- (LCP) or right-circular polarization (RCP) is able to control the polarization of the spin-VCSEL switching it at will to left- or right-circular polarization. A numerical model has been developed showing a very high degree of agreement with the experimental findings.

Spin-polarized vertical-cavity surface-emitting lasers (VCSELs) form an important class of devices in the rapidly growing field of spintronics. In these lasers, the polarization of the output emission can be controlled by utilizing the spin states of electrons in the conduction band of the active layer via the optical selection rules. This controllability of the lasing polarization offers potential applications in spin-dependent switches for optical telecommunications, reconfigurable optical interconnects, optical information and data storage, quantum computing, bandwidth enhancement, encrypted communications and biomedical sensing [1-4]. Furthermore, spin-VCSELs have unique properties such as threshold reduction, reduced wavelength chirp and the ability for independent modulation of polarization and intensity [5-8]. Spin-polarized lasers can be achieved via either an electrical injection using magnetic contacts or by photo-pumping using circularly polarized light.

Recent research advances in the spin-VCSEL have included the demonstrations of very few electrically injected 1D quantum dot, (QD) spin-VCSELs [7-10] while optically pumped spin-VCSELs have been demonstrated at short wavelength with degrees of circular polarization close to unity associated with an enhanced spin lifetime [5, 11-12]. All the latter spin-VCSELs use 2D quantum well QW active layers since it is not possible to lift the degeneracy of the spin state for 3D materials, thus no spin-VCSEL using 3D materials have been reported. Very recently, we have reported optically pumped Continuous Wave (CW) dilute nitride spin-VCSELs operating at the important telecom wavelength of 1300 nm and at room temperature [13]. In that work the polarization emitted by the spin-VCSEL could be controlled by that of the optical pump [13]. Controlling the lasing polarization by that of the pump has also been experimentally demonstrated for spin-lasers operating at shorter wavelengths [6, 14-15].

Optical injection in conventional VCSELs is commonly employed for obtaining injection locking [16-18], all-optical memory [19-22], all-optical regeneration [23] and all-optical inversion [24-27], all of which could be used to enhance the performance of the VCSELs without modifying their design. Locking and nonlinear dynamics have been studied under polarized optical injection in conventional VCSELs (parallel, orthogonal and elliptical) [28-34].

It is worth noting that circularly-polarized injection into a conventional VCSEL has not received much consideration. Most of the previous studies of optically-injected VCSELs have been focused on using linear polarized optical injection. Only Qader et al [35] have reported experiments on circularly-polarized injection into an 850 nm VCSEL; moreover a recent study has investigated theoretically the effects of different polarized optical injection (elliptical, circular or linear) in conventional VCSELs [33-34].

In addition to stable injection locking optical injection can also induce a rich variety of nonlinear dynamics in semiconductor lasers such as periodic dynamics and chaos with potentials for photonic microwave signal and chaotic sources [16-27] offering exciting prospects for applications in present and future optical systems and networks. Furthermore, as it has been previously stated, spin-polarized lasers, where the output polarization is controlled by the injection of

spin-polarized electrons, offer many attractive advantages, including polarization stability and reduced threshold current, and have potential applications in cryptographic communications and reconfigurable optical interconnects [1-8]. Hence, by combining the hitherto disparate fields of spin-lasers with optical injection the research directions described in this work open a research avenue with many routes to description of physical phenomena and potential applications.

In this letter, we combine spin-VCSEL with coherent circularly-polarized optical injection and we report investigation of an optically-injected dilute nitride spin-VCSEL emitting at the very important telecom wavelength of 1300nm and operating at room temperature. Control of the emitted polarization by the optically injected signal is experimentally demonstrated, in good agreement with numerical studies based on the spin-flip model (SFM) [34, 36-37].

Specifically, in the theoretical calculations of this work we used the SFM's extended version reported in [34] which takes into account the effect of polarized optical pumping and the spontaneous emission noise. This model includes six rate equations. These are written in terms of the amplitude and phases of the polarized electric field components denoted respectively by $E_{x(y)}$ and $\phi_{x(y)}$. The corresponding normalized carrier densities n_+ and n_-, associated respectively with spin-down and spin-up electron populations, are expressed in terms of normalized carrier variables $N = (n_+ + n_-)/2$ and $m = (n_+ - n_-)/2$. The model takes into account the spin relaxation rate (γ_s) that couples spin-up and spin-down carriers, the rates of birefringence (γ_p) and gain anisotropy (γ_a) which take into account the different (complex) refractive indices along the two orthogonal crystallographic axes and which couple the two orthogonally polarized fields. The model also includes the conventional parameters used to describe semiconductor lasers when polarization is ignored, namely the carrier recombination rate γ, the photon decay rate κ, and the linewidth enhancement factor α. In addition, normalized right- (RCP) and left-circularly polarized (LCP) pump components (η_+, η_-) are included to allow for polarized optical pumping. The six rate equations for the optically injected VCSEL can be written as [38]:

$$\frac{dE_x}{dt} = \kappa[(N-1)E_x - mE_y(\sin\Delta\phi + \alpha\cos\Delta\phi)] - \gamma_a E_x + K_{inj}E_{injx}\cos\Delta_x + \sqrt{\beta_{sp}(N+m)}\,\zeta_x(t) \quad (1)$$

$$\frac{dE_y}{dt} = \kappa[(N-1)E_y + mE_x(\alpha\cos\Delta\phi - \sin\Delta\phi) + \gamma_a E_y + K_{inj}E_{injy}\cos\Delta_y + \sqrt{\beta_{sp}(N-m)}\,\zeta_y(t) \quad (2)$$

$$\frac{d\phi_x}{dt} = \kappa\left[\alpha(N-1) + m\frac{E_y}{E_x}(\cos\Delta\phi - \alpha\sin\Delta\phi)\right] - \Delta\omega - \alpha\gamma_a + K_{inj}\frac{E_{injx}}{E_x}\sin\Delta_x \quad (3)$$

$$\frac{d\phi_y}{dt} = \kappa\left[\alpha(N-1) - m\frac{E_x}{E_y}(\alpha\sin\Delta\phi + \cos\Delta\phi)\right] - \Delta\omega + \alpha\gamma_a + K_{injy}\frac{E_{injy}}{E_y}\sin\Delta_y \quad (4)$$

$$\frac{dN}{dt} = -\gamma[N(1+E_x^2+E_y^2) - (\eta_+ + \eta_-) - 2mE_yE_x\sin\Delta\phi] \quad (5)$$

$$\frac{dm}{dt} = -\gamma_s m + \gamma(\eta_+ - \eta_-) - \gamma[m(E_x^2+E_y^2)] + 2\gamma NE_yE_x\sin\Delta\phi \quad (6)$$

where K_{inj} is the coupling rate. $\Delta\omega$ is the frequency detuning defined as the difference between angular frequency of the injected signal ω_{inj} and the intermediate frequency between those of the x-polarized ($\omega_x = \alpha\gamma_a - \gamma_p$) and y-polarized ($\omega_y = \gamma_p - \alpha\gamma_a$) modes of the solitary VCSEL. The total normalized pumping rate is defined by $\eta = \eta_+ + \eta_-$. The pump ellipticity is defined as:

$$P = \frac{\eta_+ - \eta_-}{\eta_+ + \eta_-} \quad (7)$$

E_{injx} and E_{injy} are the field amplitudes for the injected signal whereas δ_x, δ_y correspond to their phases. The two fields are related by the injection angle θ_p given by:

$$E_{injx} = E_{injy}\tan\theta_p \quad (8)$$

Without loss of generality, when the dominant mode of the VCSEL is parallel to the y-direction, we set the phase $\delta_y = 0$ and write $\delta_x = \delta$ which is included in:

$$\Delta_x = \omega_y t - \phi_x + \delta \quad (9)$$

The injection level (P_{inj}) is normalized to the linearly-polarized (LP) output of the solitary-VCSEL and can be calculated from the following equation:

$$P_{inj} = 10\log(|E_{inj}|^2/|E_{sol}|^2) \quad (10)$$

where E_{sol} defined as [39]:

$$|E_{sol}|^2 = \frac{\eta}{1-\frac{\gamma_a}{\kappa}} - 1 \quad (11)$$

The effect of spontaneous emission noise has also been included by introducing a zero mean Gaussian

noise source as in [29]. β_{sp} is the spontaneous emission factor (β_{sp} =10^{-5}) [29] and $\zeta_{x,y}$ are Gaussian white noises of zero mean value. The remaining terms $\Delta\phi$, Δ_y are given by $\Delta\phi = 2\omega_y t + \phi_y - \phi_x$ and $\Delta_y = \omega_x t - \phi_y$.

The incident polarization of the injected signal is completely described by two variables: the injection angle θ_p and the phase difference δ between the x- and y-components of the injected field. Thus, the RCP (LCP) injection cases are respectively achieved by setting θ_p = 45 and δ = 90˚ (-90˚).

In this work, we converted the Cartesian field into the corresponding circularly-polarized components using the following expressions [40]:

$$\tilde{E}_+ = \frac{\tilde{E}_x + i\tilde{E}_y}{\sqrt{2}}, \tilde{E}_- = -i\frac{\tilde{E}_y + i\tilde{E}_x}{\sqrt{2}} \qquad (12)$$

where $\tilde{E}_+$ ($\tilde{E}_-$) correspond to the RCP (LCP) fields of the VCSEL. The polarization ellipticity (degree of circular polarization) of the VCSEL is defined as [37]:

$$\varepsilon = \frac{\left|\tilde{E}_+\right|^2 - \left|\tilde{E}_-\right|^2}{\left|\tilde{E}_+\right|^2 + \left|\tilde{E}_-\right|^2} \qquad (13)$$

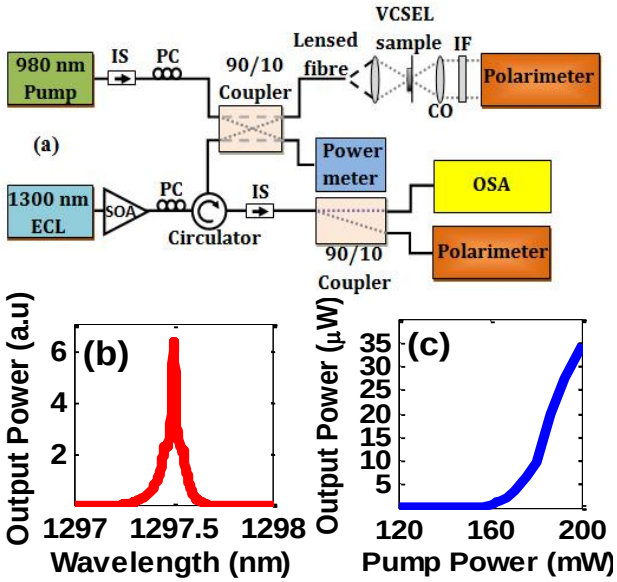

Fig1. (a) Setup used in this work to study the effect of polarized optical injection in an optically-pumped 1300 nm spin-VCSEL sample. (b) Optical spectrum of the spin-VCSEL. (c) The L-I curve under LCP pumping for the solitary spin-VCSEL with LCP output as the pump. OSA: Optical Spectrum Analyzer, SOA: Semiconductor Optical Amplifier; ECL: External Cavity Laser, IS: isolator; PC: polarization controller; IF: Interchangeable Filter, CO: collimator.

The 1300 nm dilute nitride (GaInNAs/GaAs) spin-VCSEL sample of this work consists of 16 and 20.5 GaAs/AlAs pairs forming respectively the top and bottom Bragg stacks (with estimated reflectivities of 99.2% and 99.8%) sandwiching a 3-λ cavity which includes five groups of three quantum wells (QWs) positioned approximately at the antinodes of the optical field. Each 7nm $Ga_{0.67}In_{0.33}N_{0.016}As_{0.984}$ QW was placed between 2 nm $Ga_{0.75}In_{0.25}N_{0.017}As_{0.983}$ strain mediating layers. Fig. 1 (a) presents the experimental setup used in this work to investigate the effects of optical injection on the ellipticity (ε) of the spin-VCSEL's emission (defined as in eqn. 13). The sample was pasted on a silicon carrier wafer clamped to a temperature-controlled copper mount. The mount has an opened window to allow part of the spin-VCSEL's back-side emission (transmitted through the VCSEL and silicon wafers) to be directed towards a free-space polarimeter. A 980 nm pump laser driven by a 1 A CW current source was used to optically pump the spin-VCSEL sample. The pump is connected to an isolator to avoid backward reflections and its output polarization was controlled with an in-line fibre polarization controller. 10% of the optical pump was directed to a power meter using a 90/10 coupler to monitor the CW pumping power. The other 90% was focused onto the sample using a long focal-distance lensed fiber (HI1060) which was also used to collect the spin-VCSEL sample's emission. An interchangeable optical filter is used between the free-space polarimeter and the copper mount to allow either the 980 nm pumping light or the 1310 nm spin-VCSEL emission as required. The polarization of the pump and that of the spin-VCSEL are both analyzed using the aforementioned free-space polarimeter. Under these conditions an external optical signal, generated by a 1300 nm external cavity tunable lasers (Master Laser, ML) and amplified using a semiconductor optical amplifier (SOA), is also injected into the spin-VCSEL sample via an optical circulator. The ML's output power was set to 2 mW and the SOA current was 300 mA, thus delivering 7.3 mW to the sample. A second polarization controller is used to control the ML's polarization. The third port of the circulator is followed by a 1300 nm isolator and another 90/10 coupler to direct part of the spin-VCSEL sample's light to an optical spectrum analyzer (OSA) and part to an in-line polarimeter for further analysis.

In this work we have investigated the effects of the injection strength, polarization and initial detuning of the externally injected optical signal on the ellipticity (ε) of the spin-VCSEL's emission. Previous work had experimentally demonstrated that the solitary spin-VCSEL's polarization follows that of the optical pump [13]. However, under optical injection with either RCP or LCP, the spin-VCSEL shows a different behavior as shown in fig. 2. Specifically, figs. 2(a) and 2(b) show, respectively, the experimentally measured polarization ellipticity of the spin-VCSEL's light emission as a function of the initial detuning when the device is subject simultaneously to LCP optical pumping with 180 mW and optical injection with 7 mW of either RCP (fig. 2(a)) or LCP (fig. 2(b)). Fig. 2 (a) shows that initially the spin-VCSEL's output polarization follows that of the pump; then as the ML's frequency approaches the locking bandwidth of

the solitary spin-VCSEL (the emission peak is located at 1297.51 nm as shown in fig. 1 (b)), the ML increasingly controls the polarization of the spin-VCSEL, switching it gradually from almost LCP (ε = -0.85) to RCP (ε = +1). As the detuning is increased to higher values, the polarization of the spin-VCSEL returns abruptly to LCP (ε = -0.85) being again controlled by that of the pump. Fig. 2(b) presents the case where the polarizations of the pump and the ML's injected signal are both set to LCP. It can be seen here that the optically injected signal controls the polarization of the spin-VCSEL within its locking bandwidth, achieving a high degree of LCP ($\varepsilon \approx$ -0.98).

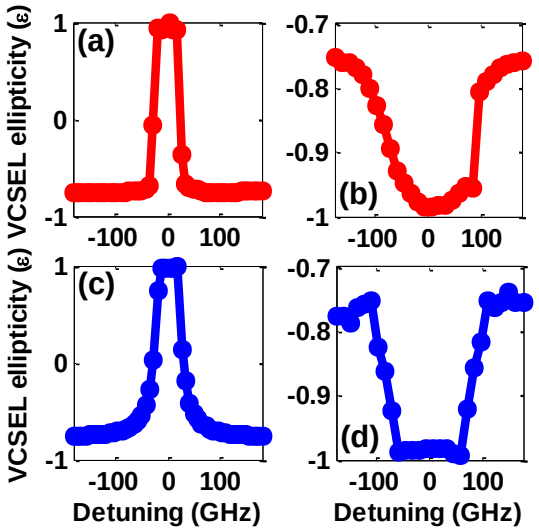

Fig. 2. Measured (a & b, in red) and calculated (c & d, in blue) output polarization of the spin-VCSEL versus detuning. The spin-VCSEL is optically-pumped with LCP light. The optically-injected signal from the ML had RCP (a & c) and LCP (b & d).

Figs. 2(c) and 2(d) plot the theoretically calculated results for the same conditions as in figs. 2(a) and 2(b).Good agreement is found between the experimental findings and the numerical calculations. The SFM parameter values used in fig 2(c) were (α =2, γ_p = 4.2 ns^{-1} , γ_s =105 ns^{-1}, η = 1.1, γ_a = 0, κ = 250 ns^{-1}, γ = 1 ns^{-1}, P_{inj} = 7 mW , K_{inj} = 43 ns^{-1}, δ = +90^o and θ_p = 42˚), while in fig 2(d) they are the same except γ_p = 4.5 ns^{-1} , K_{inj} = 148 ns^{-1} and δ = -90^o. These parameters were found by best fit to the experimental data. However, the linear anisotropies, birefringence and dichroism have not been experimentally determined due to the relatively broad spectrum of the device which does not permit the high-resolution measurements required to find these parameters. It has been experimentally and theoretically found that under the same circumstances it is much easier to lock the same helicity than the opposite one. This justifies the difference of values for some parameters such as the birefringence and the coupling rate. It is believed that the different values of birefringence arise from the strain in the sample, which changes at different positions, and hence they depend on the pumped and injected position. In fact, this also has been reported by Hendriks et al who were able to change the birefringence by applying strain to the VCSEL [41]. They fitted theory to experiment with values of 19 ns^{-1} and 6.6 ns^{-1} therein (see Figs. 2 and 5, respectively in [41]). It is also worth noting that the difference in the injection strength values refers to the coupling efficiency of the injected signal into the active region of the sample. The more the injection power coupled into the sample the higher the degree of circular polarization to be achieved.

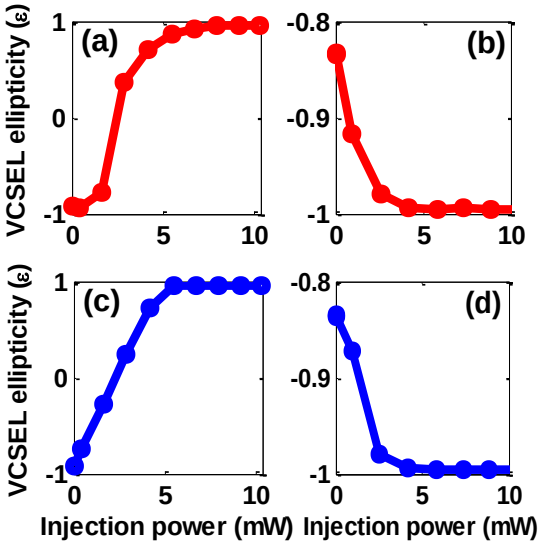

Fig. 3. Measured (a & b, in red) and calculated (c & d, in blue) output polarization of the spin-VCSEL versus optical injection strength. The spin-VCSEL is optically-pumped with LCP light. The ML's injection had RCP (a & c) and LCP (b & d).

In addition to analyzing the effect of the initial detuning we have also investigated the effect of the ML's injection strength on the polarization properties of the spin-VCSEL. It is found that when the injection strength is low, the polarization of the pump controls that of the spin-VCSEL. However, under high injection strength it is the polarization of the ML's injected signal which controls that of the spin-VCSEL. We have found that as the injection strength is increased gradual polarization switching (PS) as well as high degrees of circular polarization are achieved when the spin-VCSEL is subject to either LCP or RCP optical injection. This is illustrated graphically in the experimental plots of figs. 3(a) and 3(b) for the case of optical injection at a constant wavelength of 1297.3 nm when the solitary spin-VCSEL was pumped up to about 1.5 times the threshold (~240 mW) in both cases. The spin-VCSEL in both cases was optically-pumped with LCP light. Fig. 3(a)/ (3(c)) shows gradual PS towards very high degrees of RCP/(LCP) as the injection strength is increased. The behaviors experimentally measured in figs. 3(a) and 3(b) are in good agreement with numerical calculations using the SFM depicted in figs 3(c) and 3(d). The SFM

parameter values used in fig 3(c) were (α =2, γ_p = 3.6 ns^{-1} , γ_s =105 ns^{-1}, η = 1.5, γ_a = 0, κ = 250 ns^{-1}, γ = 1 ns^{-1}, $\Delta\omega$ = 24.8 , K_{inj} = 95 ns^{-1}, δ = -90 and θ_p = 43˚), while in fig 2(d) the difference in the following values: (α =2.9, γ_p = 4.5 ns^{-1} , η = 1.1, K_{inj} = 70 ns^{-1}, δ = -90˚ and θ_p = 38˚). The difference in injection strength is related to the coupling efficiency of the injected signal into the device, while the difference in the injection angle is related to the accuracy of the polarization controller since it needs more effort to maintain the injection angle at θ_p = 45˚all the time.

In summary, we report the experimental demonstration of optical injection into the dilute nitride 1300 nm spin-VCSEL. It has been found that the polarization of the spin-VCSEL follows that of the optical pump under low injection power whereas under high injection power the polarization of the spin-VCSEL was effectively controlled by the polarization of the ML's optically-injected signal. Moreover optical injection with circularly polarized light (RCP or LCP) produced a high degree of ellipticity in the spin-VCSEL. This behaviour is in good agreement with theoretical predictions from the spin flip model (SFM). This effective and accurate control of the polarization of the spin-VCSEL via the pump or the optical injection offers prospects for applications such as optical networks and spintronics for data encoding or for other applications where stabilized VCSEL polarization is required.

Acknowledgements

This work was funded in part by the European Union Seventh Framework Programme (FP7/2007-2013) under grant agreement no PIOF-GA-2010-273822 and by the U.K. Engineering and Physical Sciences Research Council (EPSRC) under grant reference EP/G012458/1.

References

[1] N. C. Gerhardt and M. R. Hofmann, Adv. Opt. Technol. 2012, 268949 (2012).
[2] J. Sinova and I. Žutić, Nature Mater. 11, pp.368-371 (2012).
[3] M. Holub, J. Shin, D. Saha, and P. Bhattacharya, Phys. Rev. Lett. 98, 146603 (2007)
[4] K. Ikeda, T. Fujimoto, H. Fujino, and T. Katayama, IEEE Photon. Technol. Lett., 21, 18, pp. 1350–1352 (2009)
[5] J. Rudolph, D. Hägele, H. M. Gibbs, G. Khitrova, and M. Oestreich, Appl. Phys. Lett. 82, 4516 (2003).
[6] J. Rudolph, S. Dohrmann, D. Hagele, M. Oestreich, and W. Stolz, Appl. Phys. Lett. 87, 241117 (2005).
[7] D. Basu, D. Saha, and P. Bhattacharya, Phys. Rev. Lett. 102, 093904 (2009).
[8] P. Bhattacharya, M. Holub and D. Saha, Phys. stat. sol. (c) 3, 4396 (2006).
[9] D. Saha, D. Basu, and P. Bhattacharya, Phys. Rev. B 82, 205309 (2010).
[10] D. Basu, D. Saha, C. C. Wu, M. Holub, Z. Mi, and P. Bhattacharya, Appl. Phys. Lett. 92, 091119 (2008).
[11] H. Fujino, S. Koh, S. Iba, T. Fujimoto, and H. Kawaguchi, Appl. Phys. Lett. 94, 131108 (2009).
[12] S. Iba, S. Koh, K. Ikeda, and H. Kawaguchi, Appl. Phys. Lett. 98, 081113 (2011).
[13] K. Schires, R. Al Seyab, A. Hurtado, V.-M. Korpija¨ rvi, M. Guina, I. D. Henning, and M. J. Adams, Opt. Exp., 20, 4, pp. 3550–3555 (2012).
[14] N. Gerhardt, S. Hovel, M. Hofmann, J. Yang, D. Reuter, and A. Wieck, Electron. Lett., 42, 2, pp. 88–89 (2006).
[15] S. Hövel, A. Bischoff, N. C. Gerhardt, M. R. Hofmann, T. Ackemann, A. Kroner, and R. Michalzik, Appl. Phys. Lett. 92, 041118 (2008).
[16] C.-H. Chang, L. Chrostowski, and C. J. Chang-Hasnain, IEEE J. Select. Topics Quantum Electron., 9, 5, pp. 1386–1393, (2003).
[17] L. Chrostowski, B. Faraji, W. Hofmann, M.-C. Amann, S. Wieczorek, and W. W. Chow, IEEE J. Sel. Topics Quantum Electron., 13, 5, pp. 1200–1208, (2007).
[18] A. Hurtado, D. Labukhin, I. D. Henning, and M. J. Adams, IEEE J. Sel. Top. Quantum Electron. 15(3), 585–593 (2009).
[19] J. Sakaguchi, T. Katayama, and H. Kawaguchi, Opt. Exp., 18, 12, pp. 12362–12370 (2010).
[20] T. Katayama, T. Ooi, and H. Kawaguchi, IEEE J. Quantum Electron., 45, 11, pp. 1495–1504 (2009).
[21] J. Sakaguchi, T. Katayama, and H. Kawaguchi, IEEE J. Quantum Electron., 46, 11, pp. 1526–1534 (2010).
[22] S. H. Lee, H. W. Jung, K. H. Kim, M. H. Lee, B. S. Yoo, J. Roh, and K. A. Shore, IEEE Photon. Technol. Lett., 22, 23, pp. 1759–1761 (2010).
[23] Y. Onishi and F. Koyama, IEICE Trans. Electron., E87C, 3, pp. 409–415 (2004).
[24] Y. Onishi, N. Nishiyama, C. Caneau, F. Koyama, and C. E. Zah, IEEE J. Select. Topics Quantum Electron. , 11, 5, pp. 999–1005 (2005).
[25] Y. Onishi, N. Nishiyama, C. Caneau, F. Koyama, and C. E. Zah, IEEE Photon. Technol. Lett. , 16, 5, pp. 1236–1238, (2004).
[26] K. Hasebe and F. Koyama, Jap. J. Appl. Phys. Lett., 45, 8B, pp. 6697–6703, (2006).
[27] C. F. Marki, S. Moro, D. R. Jorgesen, P. Wen, and S. C. Esener, Electron. Lett. 44, 4, pp. 292–293, (2008).
[28] J. Buesa Alt´es, I. Gatare, K. Panajotov, H. Thienpont, and M. Sciamanna, IEEE J. Quantum Electron., 42, 2, pp. 198–207,(2006).
[29] A. Valle, M. Sciamanna, and K. Panajotov, IEEE J. Quantum Electron., 44, 2, pp. 136–143, (2008).
[30] A. Hurtado, A. Quirce, A. Valle, L. Pesquera, and M. J. Adams, Opt. Exp.,18, 9, pp. 9423–9428,(2010).
[31] K. Schires, A. Hurtado, I. D. Henning, and M. J. Adams, AIP Advances,1, 3, 032131 (2011).
[32] R. Al Seyab, K. Schires, N. Khan, A. Hurtado, I. D. Henning, and M. J. Adams, IEEE J. Sel. Topics Quantum Electron.,17, 5, pp. 1242–1249, (2011).
[33] R. Al-Seyab, K. Schires, A. Hurtado, and I. Henning, M. Adams. Conference (ISLC 2012), San Diego, CA, USA (2012).
[34] R. Al Seyab, K. Schires, A. Hurtado, I. D. Henning, and M. J. Adams, IEEE J. Select. Topics Quantum Electron., 19, 4 (2013).
[35] A. A. Qader, Y. Hong and K. A. Shore, J. Lightwave Technol., 29, 24, pp. 3804-3809, (2011).
[36] M. San Miguel, Q. Feng, and J. V. Moloney, Phys. Rev. A, 52, 1728 (1995).
[37] A. Gahl, S. Balle, and M. San Miguel, IEEE J. Quantum Electron., 35, 3, pp. 342–351, (1999).
[38] R. Al-Seyab, Ph.D thesis, University of Essex, UK (2012).
[39] A. Homayounfar andM. J.Adams, Opt. Commun., 269, 1, pp. 119–127, (2007).
[40] J. Martin-Regalado, F. Pratl, M. San Miguel, and N. B. Abraham, IEEE J. Quantum Electron., 33, 5, pp. 765–783 (1997).
[41] R. F. M. Hendriks, M. P. van Exter, J. P. Woerdman, K. H. Gulden, and M. Moser, IEEE J. Quantum Electron., 34, 8, pp. 1455-1460, (1998).